AEGC Australasian Exploration Geoscience Conference | Brisbane 2023

Data analysis and interpretation of well logs in NDI Carrara 1, Northern Territory

Liuqi Wang
Geoscience Australia
liuqi.wang@ga.gov.au

Adam Bailey
Geoscience Australia
adam.bailey@ga.gov.au

Emmanuelle Grosjean
Geoscience Australia
emmanuelle.grosjean@ga.gov.au

Chris Carson
Geoscience Australia
chris.carson@ga.gov.au

Lidena K. Carr
Geoscience Australia
lidena.carr@ga.gov.au

Grace Butcher
Geoscience Australia
grace.butcher@ga.gov.au

Chris Boreham
Geoscience Australia
chris.boreham@ga.gov.au

Chris Southby
Geoscience Australia
chris.southby@ga.gov.au

Paul Henson
Geoscience Australia
paul.henson@ga.gov.au

SUMMARY

The recently drilled deep stratigraphic drill hole NDI Carrara 1 penetrates the carbonate formations of the Cambrian Georgina Basin as well as the underlying Proterozoic successions of the Carrara Sub-basin. The Proterozoic section consists predominantly of tight shales, siltstones, and calcareous clastic rocks. This study aims to assess the petrophysical properties of the Proterozoic shales using conventional wireline logs.

Gamma ray and neutron-density crossplot were used to calculate shale volume fraction, and neutron-density crossplot was applied to compute the total and effective porosity. Total organic carbon (TOC) content was interpreted using artificial neural networks, and was used to derive the volume of organic matter was converted from TOC content. Bulk density logs were corrected by removing the kerogen effect in the organic-rich shales. Matrix and kerogen densities were obtained by correlating the reciprocal of grain density with TOC content. Total shale porosity was calculated from kerogen-corrected density porosity and organic porosity. Water saturation was derived using the dual-water equation.

The Proterozoic Lawn Hill Formation in NDI Carrara 1 exhibits petrophysical properties that indicate a favourable potential for shale gas resources. Herein, we define three informal intervals within the intersected Lawn Hill Formation; the upper Lawn Hill, the Lawn Hill shale, and the lower Lawn Hill. The net shale thickness of the upper Lawn Hill and Lawn Hill shale intervals is 166.6 m and 150.3 m, respectively. The increased TOC content and organic porosity of the upper Lawn Hill and Lawn Hill shale implies higher adsorbed gas content potential. The Lawn Hill shale has the highest interpreted gas saturation (average of 33%) and the highest potential for free gas content, corresponding to the highest methane responses in logged mud gas profiles.

Key words: NDI Carrara 1, wireline log interpretation, artificial neural networks, total organic carbon content, petrophysical interpretation for shales.

INTRODUCTION

Interpretation of the L210 South Nicholson and L212 Barkly seismic surveys uncovered a large sedimentary depocentre beneath the Georgina Basin in between the greater McArthur Basin, northern Lawn Hill Platform and Mount Isa Province. This has been termed as the 'Carrara Sub-basin' by Geoscience Australia (Henson *et al.*, 2018; Carr *et al.*, 2019; Carson *et al.*, 2022) (Figure 1). The recently drilled deep stratigraphic drill hole NDI Carrara 1 penetrates the carbonate formations of the Cambrian Georgina Basin as well as the underlying Proterozoic successions of the Carrara Sub-basin. Under a regional unconformity, the Proterozoic interval consists predominantly of tight shales, siltstones, and calcareous clastic rocks in the Widdallion Sandstone and Lawn Hill Formation (Figure 2). The Lawn Hill Formation has been informally divided into three internal intervals: the lower Lawn Hill; the Lawn Hill shale; and the upper Lawn Hill (Bailey *et al.*, 2022a), and we make use of these informal units herein. Mudlog gas profiles acquired during drilling display strong gas peaks (e.g. methane peaks up to ~1.6×10^5 ppm) in the Lawn Hill shale interval.

During logging of NDI Carrara 1, compact gamma ray, photodensity, borehole-compensated neutron porosity, array induction and shallow-focused resistivity, cross-dipole sonic and high-resolution spectral gamma ray logs were collected (Figure 2), and these logs were used for interpretation of the volume fraction of shale, total and effective porosities for the Proterozoic succession using conventional, established methods. This was followed by a neural network based

interpretation of total organic carbon (TOC) content, density porosity and water saturation interpretations for the Proterozoic shale reservoirs.

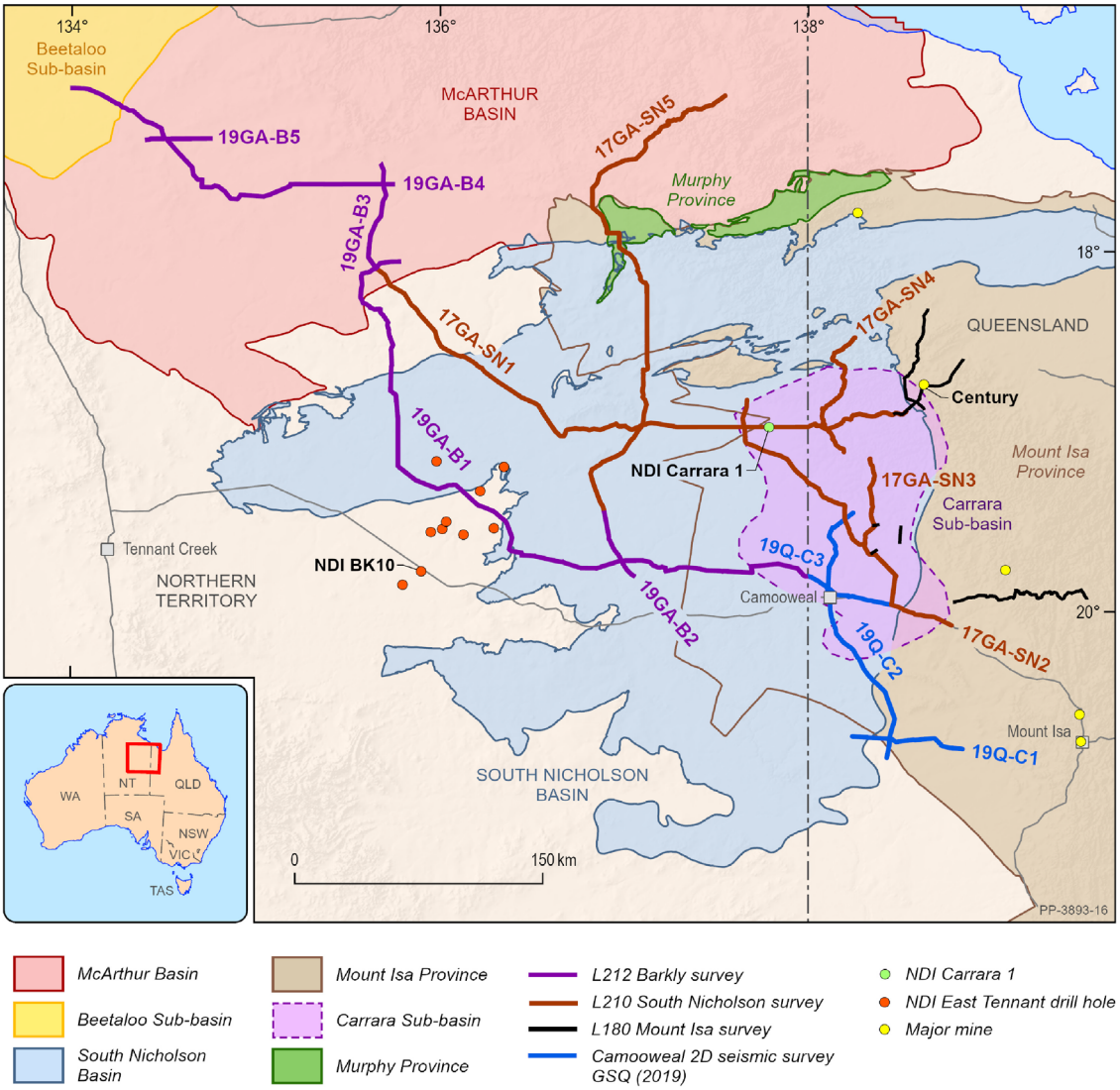

Figure 1. Location of the NDI Carrara 1 stratigraphic drillhole and deep crustal reflection seismic survey lines across the McArthur Basin, South Nicholson Basin and Carrara Sub-basin (Carson *et al.*, 2022).

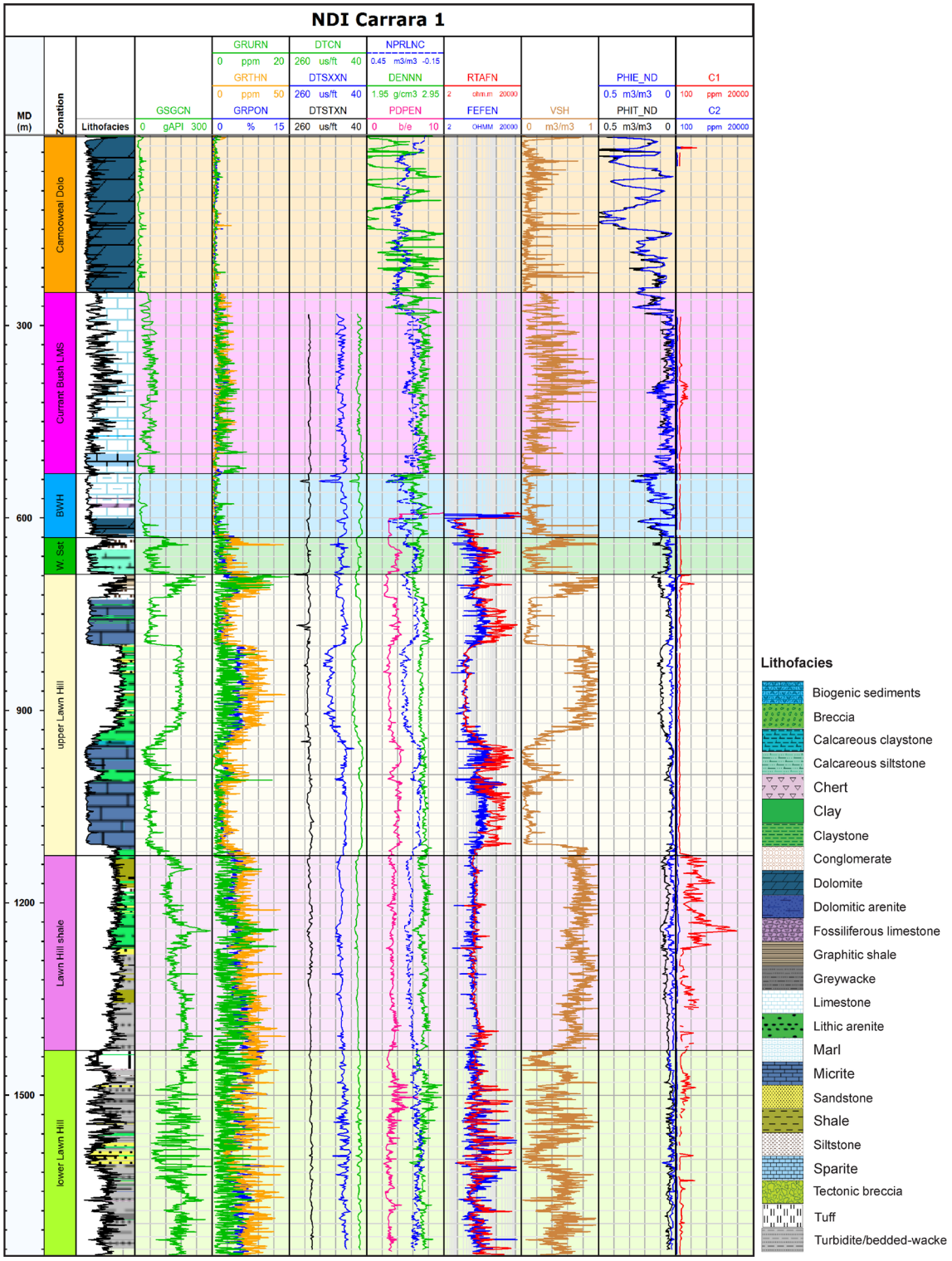

Figure 2. Well logs and conventional interpretation results of NDI Carrara 1. From left to right, Track 1: Driller's depth below ground floor (MD, m); Track 2: Stratigraphic units; Track 3: Lithological sequence; Track 4: High-resolution spectral gamma ray (GSGCN, gAPI); Track 5: Concentration logs of uranium (GRURN, ppm), thorium (GRTHN, ppm) and potassium (GRPON, %) from spectral gamma ray tool; Track 6: Compressional, shear and Stoneley wave slowness (DCTN, DTSXXN and DTSTXN, μs/ft); Track 7: Bulk density (DENNN, g/cm^3), limestone neutron porosity (NPRLNC, m^3/m^3) and photoelectric factor (PDPEN, b/e); Track 8: Deep and shallow resistivity (RTAFN and FEFEN, ohmm); Track 9: Volume fraction of shale (VSH, m^3/m^3); Track 10: Total and effective porosity (PHIT_ND and PHIE_ND, m^3/m^3); Track 11: Concentrations of methane and ethane from mudlog (C1 and C2, ppm). W.SST = Widdallion Sandstone Member, BWH = Border Waterhole Formation.

VOLUME FRACTION OF SHALE AND NEUTRON-DENSITY POROSITY

Conventional interpretation includes the volume fraction of shale (V_{shale}), total and effective porosity for the Cambrian successions. V_{shale} was calculated from gamma ray logs using Larionov model for the Cambrian successions, and neutron-density crossplots for the Proterozoic successions. Total and effective porosity were calculated using traditional neutron-density crossplot (Schlumberger 2013).

Water saturation interpretation was not conducted for the Cambrian successions due to the lack of resistivity data However, it is worth noting that the mudlog gas profiles through the Georgina Basin interval has methane concentration peaks within the Current Bush Limestone from 386.9–423.5 m with an average value of 3275 ppm, associated with interpreted high TOC and porosity (Figure 2). This interval is likely to be of further interest as a potential source rock and/or unconventional play (Figure 2).

This study was focused on assessing the petrophysical properties of the Proterozoic shales using conventional wireline logs. Mudlog gas profiles show that the Proterozoic Lawn Hill Formation has typically shale dry gas reservoirs (methane concentration > 85%). The rock constituents of shales were assumed to have non-clay and clay minerals, organic matter and formation fluids (gas and water). Well log interpretations aimed to improve the interpretations of organic porosity, total density porosity and water saturation followed by total organic carbon (TOC) content interpretation from well logs.

TOTAL ORGANIC CARBON CONTENT

Total organic carbon (TOC) content indicates the richness of organic matter in sedimentary rocks, which is a critical parameter for assessing the hydrocarbon generation potential of source rocks and the adsorbed gas content of shales. The presence of organic matter may increase the resistivity, lower the bulk density and increase the transmission time of acoustic waves (Schmoker and Hester, 1983; Passey *et al.*, 1990). Radioactive log values may also be increased since organic-rich shales have the ability to absorb radioactive elements from aqueous solution (Schmoker, 1981; Schlumberger 2013). Total organic carbon content was correlated with and estimated from conventional well log data, such as radioactive logs, porosity logs and resistivity logs (Schmoker, 1981; Schmoker and Hester, 1983; Passey *et al.*, 1990). Artificial neural network learning (Wang *et al.*, 2021 and 2022) was employed to learn the relationships between wireline logging data and TOC content, thereby approximating TOC content from well logs.

Neural Network Interpretation

Artificial neural networks (ANNs) approach with multiple hidden layers was employed to interpret the TOC content from well logs (Mebsout, 2020; Roberts *et al.* 2022; Wang *et al.*, 2022). The estimation of TOC content was performed in two steps. Firstly, training patterns, including both input (well logs) and output (laboratory measured TOC content) parameters, were presented to train the neural networks. Secondly, well logs from unsampled intervals were imported into the trained ANNs model to derive approximated TOC content.

In NDI Carrara 1, a total of 254 samples from the Proterozoic successions were analysed by Rock-Eval pyrolysis to obtain the TOC content (Butcher *et al.*, 2021). The input well logs included the total gamma ray, uranium, thorium and potassium concentrations from spectral gamma ray logs, neutron porosity, bulk density, compressional sonic wave slowness and logarithmic deep resistivity logs, plus one output parameter of laboratory measured TOC content. During the neural network learning process, min-batch gradient was used to optimise the weights and biases. Grid search approach was applied to find the optimal hyperparameters, such as the number of hidden layers and neurons, activation function, learning rate and batch size (Roberts *et al.*, 2022; Wang *et al.*, 2022). The number of testing patterns was set as 15% of all patterns. The correlation coefficient (R^2) between laboratory measurements and neural network approximations is 0.8428.

Net Shale Thickness

Organic-rich shales were identified where TOC content is greater than 1 wt% in the neural network interpreted TOC content profiles, and this was used to calculate a net shale ratio for each unit. The net shale ratio was defined as the ratio of net shale thickness (TOC>1 wt%) over gross formation thickness. No organic-rich shale was interpreted in the Widdallion Sandstone or the lower Lawn Hill. Calculated net shale ratios for the upper Lawn Hill and Lawn Hill shale are 0.380 and 0.495, respectively. These ratios correspond to net shale thickness of 166.6 m and 150.3 m within the upper Lawn Hill and Lawn Hill shale, respectively.

PETROPHYSICAL PROPERTY OF SHALES

It is challenging to interpret the total porosity in shale gas reservoirs because of the fine-grained texture, low porosity, ultra-low permeability, and high content of organic matter and clay minerals. In a shale reservoir, organic matter behaves like porosity to logged bulk density, and it is necessary to remove this effect in order to derive a reliable total porosity for shale reservoirs.

Volume of Organic Matter

The Proterozoic, organic-rich shale rocks in NDI Carrara 1 are predominantly over-mature according to bitumen reflectance measurements and conversions to equivalent vitrinite (Ranasinghe and Crosdale, 2022; Grosjean *et al.*, 2022). These shales were deposited in a marine environment (Crombez *et al.*, 2022), and the organic matter was likely associated with type II kerogen or a mixture of type I and II kerogen. For the purpose of porosity interpretation, the volume of organic matter was firstly converted from TOC content (Tissot and Welte, 1984; Peters *et al.*, 2005):

$$V_{OM} = \frac{\gamma \times TOC \times \rho_b}{100 \times \rho_{OM}},$$

where V_{OM} is the organic matter (kerogen) volume fraction (fractions); TOC is total organic carbon content (wt%); ρ_b is the rock bulk density (g/cm^3); ρ_{OM} is the density (g/cm^3) of organic matter, ranging from 1.1 to 1.4 g/cm^3; γ is the conversion factor from TOC to organic matter (Tissot and Welte 1984), which is dependent on kerogen type and thermal maturity.

Thirty two samples from the Proterozoic successions were tested for grain density, total and gas porosity (Bailey *et al.*, 2022b). Figure 3 presents the plotted reciprocal of laboratory measured grain density against the neural network interpreted TOC contents. The density of organic matter (ρ_{OM}) was estimated to be 1.28 g/cm^3 where TOC content = 100 wt%, and the matrix density was 2.78 g/cm^3 where TOC content = 0 wt% (Figure 4). The matrix density of shale was estimated from this relationship as follows:

$$\rho_{ma} = 1/(0.0042 \times TOC + 0.3599).$$

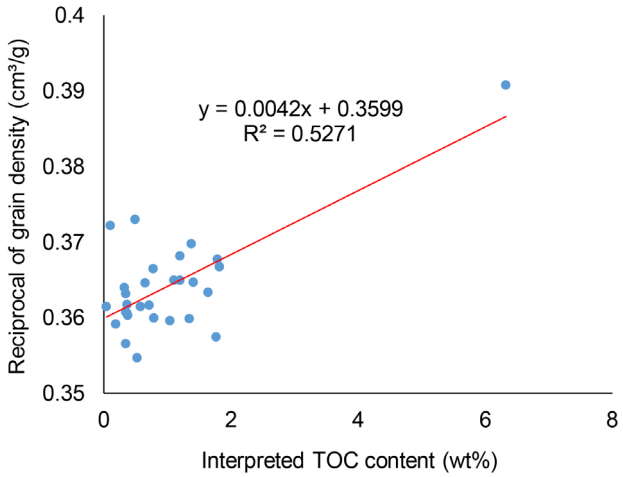

Figure 3. Plot of reciprocal of the laboratory measured grain density versus neural network interpreted TOC content.

Organic Matter-Corrected Density Porosity

Bulk density log was corrected by removing the effect of organic matter as follows:

$$\rho_{bkc} = \frac{\rho_b - \rho_{OM} \times V_{OM}}{1 - V_{OM}}.$$

The organic matter corrected density porosity was derived by:

$$\phi_{kc} = \frac{\rho_{ma} - \rho_{bkc}}{\rho_{ma} - \rho_{fl}},$$

where ρ_{OM} is the density of organic matter (g/cm^3); V_{OM} is the volume fraction of organic matter (fractions); ρ_{bkc} is the organic matter corrected bulk density (g/cm^3); ρ_b, ρ_{ma} and ρ_{fl} are the densities of bulk density logs, matrix and fluids, respectively. ρ_{ma} was derived from the relationship in Figure 3 for shales. ϕ_{kc} is the density porosity (fractions) using corrected bulk density logs.

Organic Porosity

Organic matter has abundant pores for gas storage. It has been a challenge to estimate the porosity in organic matter using commonly used routine core analysis or petrophysical technique (Modica and Lapierre 2012; Kuchinskiy 2013). The mass-balance equation provided by Modica and Lapierre (2012) was used to compute the porosity of organic matter in the Proterozoic shales in NDI Carrara 1:

$$\phi_{OM} = ([TOC_O \times C_c] \times \gamma)TR\frac{\rho_b}{\rho_{OM}},$$

where ϕ_{OM} denotes the porosity of organic matter (fractions); TOC_O is the original TOC content (weight fraction) before maturization; C_c is the convertible carbon fraction; ρ_b and ρ_{OM} are the densities of rock and organic matter (g/cm^3); and TR is the transformation ratio and dependent on kerogen type and thermal maturity.

TOC_O, TR and C_c were calculated as follows (Peters *et al.*, 2005; Modica and Lapierre, 2012):

$$TOC_O = \frac{TOC_p}{1-TR\times C_c},$$

$$TR = 1 - \frac{HI_p[1200-HI_O(1-PI_o)]}{HI_o[1200-HI_p(1-PI_p)]},$$

$$C_c = 0.085 \times HI_O,$$

where TOC_p is the present day TOC content (weight fraction); HI_o and HI_p are the original and present hydrogen index respectively (mg/g); PI_o and PI_p are the original and present production index, respectively (S1/S1+S2). HI_p and PI_p are calculated from Rock Eval pyrolysis testing results (Butcher *et al.*, 2021).

Total Density Porosity

Total density porosity was estimated as the sum of organic matter-corrected density porosity and organic porosity.

Water Saturation

Formation water saturation was estimated from porosity and deep resistivity logs using Pickett plotting, and total water saturation (SWT_DW, pore volume fraction) was computed using the dual-water equation (Schlumberger 2013). The total gas saturation (SGT, pore volume fraction) was derived from total water saturation ($SGT = 1 - SWT\_DW$), and the gas-filled porosity was the product of total density porosity and total gas saturation (PHIGF, bulk volume fraction in Figure 4).

The results of above interpretations are presented in Figure 4, and Table 1 lists the average parameters in the Proterozoic successions in NDI Carrara 1. Lawn Hill shale and upper Lawn Hill intervals have high TOC content and organic porosity, which implies higher adsorbed gas content potential. The Lawn Hill shale interval has the lowest average water saturation of 0.67 with the minimum of 0.12. The average gas saturation is 0.33 or 33% with the maximum of 0.88 or 88%, which indicates the Lawn Hill shale interval has the highest potential for free gas content. This also corresponds to the highest methane responses in mudlog gas profiles (Table 1).

Figure 4 presents the results of the petrophysical interpretations undertaken in this study. The Lawn Hill shale and upper Lawn Hill interval have elevated TOC content and organic porosity, which implies an increased potential for elevated adsorbed gas contents. The average gas saturation of the organic-rich shales in the Lawn Hill shale is 0.49. These characteristics indicate that the Lawn Hill shale has the highest potential for free gas content of the units intersected by NDI Carrara 1. This supposition is supported by the mudlog gas profiles, where the highest methane responses are observed within the Lawn Hill shale (Table 1, Figure 4). The gas saturation of the lower Lawn Hill is 9%, which implies the gas potential of the tight non-organic-rich shales.

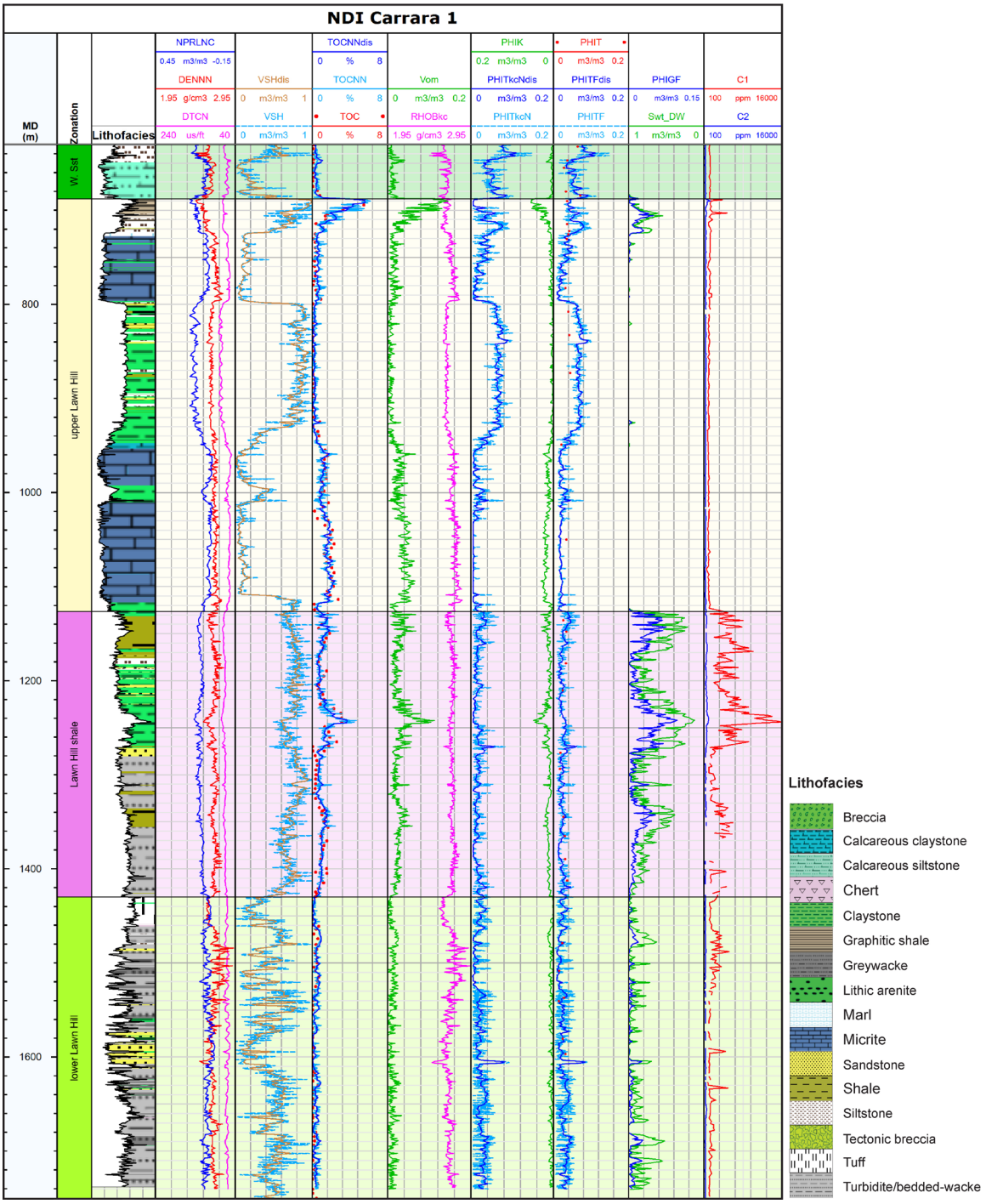

Figure 4. Petrophysical interpretation results for the Proterozoic unconventional gas reservoirs in NDI Carrara 1. From left to right, track 1: Driller's depth below ground floor (MD, m); Track 2: Stratigraphic units; Track 3: Lithological sequence; Track 4: Compressional wave slowness (DCTN, µs/ft), bulk density (DENNN, g/cm^3), limestone neutron porosity (NPRLNC, m^3/m^3); Track 5: Volume fraction of shale and its smoothed curve (VSH and VSHdis, m^3/m^3); Track 6: Laboratory measured, neural network interpreted TOC content and its smoothed curve (TOC, TOCNN, TOCNNdis, wt%); Track 7: Volume fraction of organic matter (Vom, m^3/m^3) and corrected bulk density (RHOBkc, g/cm^3); Track 8: Organic porosity (PHIK, m^3/m^3), total porosity from corrected bulk density and its smoothed curve (PHITkcN and PHITkcNdis, m^3/m^3); Track 9: Laboratory measured, interpreted total porosity and its smoothed curve (PHIT, PHITF, PHITFdis, m^3/m^3); Track 10: Water saturation and gas-filled porosity (SWT_DW and PHIGF, m^3/m^3); Track 11: Concentrations of methane and ethane from mudlog (C1 and C2, ppm).

Parameter	Widdallion Sandstone	upper Lawn Hill	Lawn Hill shale	lower Lawn Hill
TOC content (wt%)	0.41	0.97	1.10	0.39
Volume fraction of organic matter (m^3/ m^3)	0.01	0.02	0.03	0.01
Bulk density (g/cm^3)	2.64	2.67	2.68	2.68
Organic matter corrected density (g/cm^3)	2.65	2.71	2.72	2.69
Porosity with corrected density (m^3/ m^3)	0.060	0.033	0.016	0.022
Organic porosity (m^3/ m^3)	0.004	0.010	0.013	0.005
Total porosity (m^3/ m^3)	0.063	0.040	0.025	0.025
Water saturation (pore volume fraction)	1.00	0.98	0.67	0.91
Methane concentration (ppm)	1370	1100	5427	2159
Ethane concentration (ppm)	385	424	589	392

Table 1. Average petrophysical parameters in the Proterozoic succession in NDI Carrara 1.

CONCLUSIONS

This study presents the results of total organic carbon content and petrophysical property interpretations on the logging data from the deep stratigraphic drill hole NDI Carrara 1, the first stratigraphic test of the recently uncovered Carrara Sub-basin of the Northern Territory and northwest Queensland. The interpretation workflow from TOC content to porosity and water saturation interpretation has been used to conduct the integrated well log evaluation for shale gas reservoirs. The interpretation carried out herein implies that the Proterozoic Lawn Hill Formation, as intersected in NDI Carrara 1, host organic-rich shales with likely favourable for shale gas. The calculated net thickness of organic-rich shales in the upper Lawn Hill and Lawn Hill shale units is 166.6 m and 150.3 m, respectively. The shales within the upper Lawn Hill and Lawn Hill shale units have elevated TOC contents and organic porosity, implying that they are likely to have elevated levels of adsorbed gas. The Lawn Hill shale interval has the highest average gas saturation (0.33 or 33%), and the average gas saturation of the organic-rich shales in this interval is 0.49, which indicates the highest potential for free gas content. The lower Lawn Hill has gas potential in the tight non-organic-rich shales. The free gas potential corresponds to the highest measured methane responses in the mudlog gas profile.

ACKNOWLEDGMENTS

This study was funded by Geoscience Australia's Exploring for the Future program. We thank Dianne Edwards and Duy Nguyen for internal peer reviews at Geoscience Australia. This paper is published with the permission of the CEO, Geoscience Australia.

REFERENCES

Bailey, A.H.E., Wang, L., Grosjean, E., Carson, C.J., Butcher, G., Jarrett, A.J., and Henson, P., 2022a, New geomechanical and petrophysical data from NDI Carrara 1; implications for Carrara Sub-basin unconventional prospectivity. Central Australian Basins Symposium IV (CABS IV), Darwin, Northern Territory, 29-30 August 2022.

Bailey, A.H.E., Wang, L., Carson, C.J., Dewhurst, D.N., Esteban, L., Kager, S., Monmusson, L., Crombez, V., Delle Piane, C., Nguyen, D., and Henson, P., 2022b, Exploring for the Future – petrophysical testing program data release - NDI Carrara 1, Carrara Sub-basin, Australia: Geoscience Australia, Canberra. https://dx.doi.org/10.26186/147234.

Butcher, G., Grosjean, E., Jarrett, A.J., Boreham, C.J., Jinadasa, N., Webster, T., Hong, Z., Carson, C.J., 2021, Exploring for the Future - Rock-Eval pyrolysis data from NDI Carrara 1, South Nicholson region, Australia: Data Release Record 2021/26. Geoscience Australia, Canberra.

Carr, L.K., Southby, C., Henson, P.A., Carson, C.J., Anderson, J.R., MacFarlane, S., Jarrett, A.J.M., Fomi,n T., and Costelloe, R., 2019, Exploring for the Future: South Nicholson Basin region project outcomes and sequence stratigraphy: Annual Geoscience Exploration Seminar (AGES) Proceedings, Alice Springs, Northern Territory.

Carson, C.J., Kositcin, N., Henson, P. A., Delle Piane, C., Crombez, V., Grosjean, E., Jarrett, A.J.M., and Butcher, G., 2022, Exploring for the Future - SHRIMP U–Pb zircon geochronology from NDI Carrara 1 and implications for regional stratigraphic correlations, resource potential and geological evolution of the Carrara Sub-basin: Annual Geoscience Exploration Seminar (AGES) 2022 Proceedings, NT Geological Survey, 27-36.

Crombez, V., Delle Piane, C., Dewhurst, D., 2022, NDI Carrara 1 sedimentology, microstructural analyses, and sequence stratigraphy. Geoscience Australia – FINAL REPORT: Geoscience Australia, Canberra. https://dx.doi.org/10.26186/147247.

Curtis, J. B., 2002, Fractured shale-gas systems: AAPG Bulletin, 86, 2002.

Grosjean, E., Jarrett, A., Boreham, C., Butcher, G., Carson, C., Bailey, A., Wang, L., Munson, T., and Henson, P., 2022, The energy resource potential of the Carrara Sub-basin revealed by new stratigraphic drilling. *AGES* 2022. 5-6 April 2022, Alice Springs, NT Geological Survey. pp. 75-83.

Henson, P., Carr, L., Fomin, T., Gerner, E., Costelloe, R., Southby, C., Anderson, J., Bailey, A., Lewis, C., Champion, D. and Huston, D., 2018, Northern Territory Geological Survey and Queensland Geological Survey, 2018. Exploring for the Future: Discovering the South Nicholson Basin region with new seismic data: Annual Geoscience Exploration Seminar (AGES) 2018 Record of Abstracts. Northern Territory Geological Survey, Darwin. 52–54.

Kuchinsky, V., 2013, Organic porosity study: Porosity development within organic matter of the Lower Silurian and Ordovician source rocks of the Poland shale gas trend: AAPG Annual Convention and Exhibition, Pittsburgh, Pennsylvania, May 19-22, 2013.

Modica, C.J., and Lapierre, S.G., 2012, Estimation of kerogen porosity in source rocks as a function of thermal transformation: Example from the Mowry Shale in the Powder River Basin of Wyoming: AAPG Bulletin, 96(1), 87–108.

Passey, Q., Creaney, S., Kulla, J., Moretti, F., and Stroud, J., 1990, A practical model for organic richness from porosity and resistivity logs: AAPG Bulletin, 74, 1777–1794.

Peters, K.E., and Walters, C., 2005, Moldowan, J.M. Biomarkers and Isotopes in the Environment and Human History: Cambridge University Press, Cambridge, UK.

Ranasinghe, S.P., and Crosdale, P.J., 2022, Source rock type, maturation levels and hydrocarbon potential in a suite of samples from NDI Carrara 1 drill hole, Northern Territory: Geoscience Australia Record 2022.

Roberts, D., Yaida, S., & Hanin, B., 2022., The Principles of Deep Learning Theory: An Effective Theory Approach to Understanding Neural Networks: Cambridge University Press, Cambridge, UK. doi:10.1017/9781009023405.

Schlumberger, 2013, Schlumberger Log Interpretation Charts. 2013 Edition: ©Schlumberger 1991, Schlumberger Wireline and Testing, Texas, USA.

Schmoker, J.W., 1981, Determination of organic-matter content of Appalachian Devonian shales from gamma-ray logs: AAPG Bulletin, 65, 1285–1298.

Schmoker, J.W., and Hester, T.C., 1983, Organic carbon in Bakken Formation, United States portion of Williston Basin: AAPG Bulletin, 67, 2165–2174.

Tissot, B.P., and Welte, D.H., 1984, Petroleum Formation and Occurrence: 2nd edition: Springer-Verlag, Berlin.

Wang, L., Edwards, D.S., Bailey, A., Carr, L.K., Boreham, C.J., Grosjean, E., Normore, L., Anderson, J., Jarrett, A. J.M., McFarlane, S., Southby, C., Carson, C., Khider, K., and Henson, P., 2021, Petrophysical and geochemical interpretations of well logs from the pre-Carboniferous succession in Waukarlycarly 1, Canning Basin, Western Australia: The APPEA Journal, 61(1), 253–270.

Wang, L., Bailey, A., Carr, L.K., Edwards, D.S., Khider, K., Anderson, J., Boreham, C.J., Southby, C., Dewhurst, D., Esteban, L., Munday, S., and Henson, P., 2022, Petrophysical characterisation of the Neoproterozoic and Cambrian successions in the Officer Basin: The APPEA Journal, 62(1), 381–399.